Pax6 Overexpression Suppresses Cell Proliferation and Retards the Cell Cycle in Corneal Epithelial Cells

Jie Ouyang,[1,2,3] *Ying-Cheng Shen,*[3,4] *Lung-Kun Yeh,*[5] *Wei Li,*[1] *Brad M. Coyle,*[1] *Chia-Yang Liu,*[1,6] *and M. Elizabeth Fini*[1,2,6]

Purpose. The gene encoding transcription factor *Pax6* resides at the top of a genetic hierarchy controlling development and morphogenesis of the eye. Pax6 continues to be expressed in the ocular surface epithelia of the postnatal eye. The goal of this study was to investigate a possible role for *Pax6* in controlling dynamics of the ocular surface epithelia.

Methods. Full-length mouse *Pax6* (*mPax*) cDNA, or truncated *mPax6Δ286* lacking the transcriptional activation domain was inserted into a tetracycline-inducible vector (Tet-on). A rabbit corneal epithelial cell line SIRC was used to establish stable transformants. Induction of Pax6 or truncated Pax6Δ286 proteins by doxycycline (DOX) was examined by Western blot and immunohistochemistry. The effects of Pax6 overexpression on cell cycle progression were assessed by the cell proliferation index, cell growth curve, and cell cycle assay. Terminal deoxynucleotidyl transferase biotin-dUTP nick end labeling (TUNEL) assay was performed to detect apoptotic cells. Recombinant adenovirus-carrying *mPax6* or *mPax6Δ286* transgenes were used for transient transduction of primary rabbit corneal epithelial cells, and the effect on cell cycle progression was assayed.

Results. The level of Pax6 or truncated Pax6 was tightly regulated by DOX. Overexpression of full-length Pax6 retarded the rate of cell proliferation, whereas the truncated form had no effect. Full-length Pax6 affected the rate at which individual cells traversed the cell cycle and induced caspase-3-independent apoptosis in a small percentage of cells. Transient transduction of cells with recombinant *mPax6* adenovirus also inhibited cell proliferation.

Conclusions. Inhibition of cell proliferation in *Pax6*-overexpressing corneal epithelial cell lines and primary cell culture is consistent with the notion that *Pax6* plays a role in controlling corneal epithelial cell dynamics in vivo. (*Invest Ophthalmol Vis Sci.* 2006;47:2397–2407) DOI:10.1167/iovs.05-1083

The ocular surface constitutes the epithelial sheets that cover the cornea and conjunctiva.[1] These tissues are specialized in a variety of ways to facilitate sliding of the eyelids and protection of the eye. The epithelial sheets are established in the embryo, but (like all epithelia) the postnatal tissues constantly undergo self-renewal and can regenerate completely after injury.[2,3] These renewal processes are critical, as defects in the ocular surface epithelium can lead to corneal melting, scarring, and blindness.[4,5] Much still needs to be learned about how ocular surface epithelia develop and are maintained, including understanding the processes controlling cell proliferation, cell differentiation, cell migration, and cell death.[6–9]

The gene encoding transcription factor *Pax6* resides at the top of a genetic hierarchy controlling development and morphogenesis of the eye.[10–13] *Pax6* is a highly conserved member of a family of genes encoding transcription factors that contain two DNA-binding domains—the paired domain (PD) and the homeodomain (HD)[14]—and a transcriptional activation domain.[15] Mutations in *Pax6* are the basis of Drosophila *eyeless* and rodent *small eye* (SEY) phenotypes. In rodents, homozygosity for these loss-of-function mutations is lethal and includes brain defects and a complete absence of eyes.[16] Heterozygosity (haploinsufficiency) for *Pax6* in mice or humans is associated with a spectrum of eye defects, depending on the location of the mutation within the *Pax6* gene. Of note, increased *Pax6* gene dosage in transgenic mice causes developmental abnormalities of the eye similar to those associated with haploinsufficiency.[17] This suggests that cells are exquisitely sensitive to changes in levels of *Pax6* activity in either a positive or negative direction.

Pax6 is expressed in various tissues of the anterior segment and retina during development. It is also prominently expressed in the ocular surface epithelia of the adult.[18] Most human eye disorders resulting from haploinsufficiency for *Pax6* involve anterior chamber structures, including the iris and cornea.[19–21] Two strains of SEY mice examined in detail have revealed abnormal corneal morphology, especially in the epithelium.[22] These observations suggest that *Pax6* is involved in development of the ocular surface epithelia. Indeed, correct *Pax6* dosage during eye development in SEY mice has been shown to influence clonal growth of corneal epithelial cells, stem cell activity, and epithelial cell migration.[23]

Pax6 is also expressed in the postnatal corneal epithelium, and protein levels and DNA binding activity of Pax6 are increased at the front of corneal epithelium migrating to close a wound.[23] Therefore, it seems likely that *Pax6* controls corneal epithelial dynamics in the adult much as during development; however, studies to investigate this question using SEY mice are confounded by the effects of *Pax6* deficiency on tissue

From the [1]Bascom Palmer Eye Institute and the [2]Graduate Program in Physiology and Biophysics, Miller School of Medicine, University of Miami, Miami, Florida; the [4]Department of Ophthalmology, Veterans General Hospital, Taichung, Taiwan, Republic of China; and the [5]Department of Ophthalmology, Chang Gung Memorial Hospital, Linko, Taiwan, Republic of China.

[3]Contributed equally to the work and therefore should be considered equivalent authors.

[6]Contributed equally to the work and should be considered equivalent senior authors.

Supported by National Eye Institute (NEI) R01 Project Grants EY012651 (MEF) and EY012486 (C-YL), a P30 core Grant EY014801 (MEF), and an unrestricted grant from Research to Prevent Blindness (RPB). C-YL was the 2004 RPB Olga Keith Wiess Special Scholar. MEF was a 2005 RPB Senior Scientific Investigator and holds the Walter G. Ross Chair in Ophthalmic Research.

Submitted for publication August 16, 2005; revised January 20, 2006; accepted April 21, 2006.

Disclosure: **J. Ouyang**, None; **Y.-C. Shen**, None; **L.-K. Yeh**, None; **W. Li**, None; **B.M. Coyle**, None; **C.-Y. Liu**, None; **M.E. Fini**, None

The publication costs of this article were defrayed in part by page charge payment. This article must therefore be marked "*advertisement*" in accordance with 18 U.S.C. §1734 solely to indicate this fact.

Corresponding author: M. Elizabeth Fini, Bascom Palmer Eye Institute, Miller School of Medicine, University of Miami, 1638 NW 10th Avenue, Miami, FL 33136; efini@med.miami.edu.

development and by the complexity of tissue interactions in vivo.

In this study, we investigated the mechanism whereby *Pax6* modulates corneal epithelial cell growth by studying the effects of overexpression in a cultured rabbit corneal epithelial cell line. Stably transformed cell lines were created and cloned to obtain pure cell populations for study. To avoid any confounding effects on cell growth or survival due to *Pax6* expression during clonal expansion, we used the tetracycline-inducible gene expression (Tet-On) system.[24] To address biological relevance, we also examined the effects of overexpression in primary cultures of rabbit corneal epithelial cells, using the efficient adenoviral-mediated transfection method.

Materials and Methods

Corneal Epithelial Cell Culture

The rabbit corneal epithelial cell line, SIRC (CCL-60; American Type Culture Collection, Manassas, VA), was cultured in minimum essential medium (MEM) supplemented with 10% fetal bovine serum (Invitrogen, Carlsbad, CA).

To obtain primary epithelial cells for culture, fresh New Zealand rabbit eyes were purchased from Pelfreez (Rogers, AR), and corneas were excised and placed in 100-mm plates filled with 1% dispase (Invitrogen) in keratinocyte-SFM (KSFM; Invitrogen) at 4°C overnight. The next day, the epithelial cells were removed by gentle scraping with a scalpel, resuspended in 0.05% trypsin-EDTA and incubated at 37°C for 30 minutes; resuspended in KSFM with 10% FBS, penicillin/streptomycin (Invitrogen); and amphotericin B (Sigma-Aldrich, St. Louis, MO); counted; and plated in 100-mm culture dishes.

Plasmids and Stable Transfection

To enable us to increase the expression level of *Pax6* in SIRC cells on demand, we created stably transformed the SIRC cell lines, employing the Tet-On system.[24]

The mouse *Pax6* cDNA template was kindly provided by Joram Piatigorsky (National Eye Institute, Bethesda, MD)[25] and amplified by polymerase chain reaction (PCR) (primer 1: 5′-TCC ACG CGT ATG CAG AAC AGT CAC AGC GGA; primer 2: 5′-TCC ACG CGT TTA CTG TAA TCG AGG CCA GTA). A truncated form of *Pax6*, *mPax6Δ286* (the N-terminal 286 amino acids without the PST domain responsible for transcriptional activation), was also generated by PCR (primer 1: 5′-TCC ACG CGT ATG CAG AAC AGT CAC AGC GGA; primer 2: 5′-TCC ACG CGT TTA AGG AAT GTG ACT AGG AGT GTT GCT). Evidence has been presented that this fragment acts as a dominant-negative inhibitor of full-length Pax6 activity.[25] The cDNA fragments were cloned into the *Mlu*I sites of the multiple cloning site (MCS) of the plasmid *pBI-EGFP* (BD-Clontech, Palo Alto, CA) to generate *pBI-EGFP-Pax6* and *pBI-EGFP-Pax6Δ286* (Fig. 1A). All constructs were verified by nucleotide sequencing in the DNA core laboratory of the University of Miami Miller School of Medicine.

SIRC cells were cotransfected with 10 μg *pBI-EGFP-Pax6* or *pBI-EGFP-Pax6Δ286* and 1 μg *pTet-On* (BD-Clontech) using transfection reagent (Gene Jammer; Stratagene, La Jolla, CA) according to the manufacturer's instructions (the vector contains the gene for resistance to the geneticin antibiotic to enable selection of stably transformed cells). Stably transfected colonies were selected in medium containing 1000 μg/mL geneticin (G418; Invitrogen) for 10 to 14 days.

The *pBI-EGFP-Pax6* and *pBI-EGFP-Pax6Δ286* drives transcription bidirectionally to produce Pax6 or Pax6Δ286, and enhanced green fluorescent protein (EGFP) when rtTA, the product of *pTet-On*, is activated and binds to the tetracycline-responsive element (TRE). Thus, the resultant colonies were treated with 1 μg/mL of doxycycline (DOX; BD-Clontech) for 24 hours and screened under a microscope equipped for epifluorescence using the FITC filter. Colonies exhibiting strong green fluorescence in the cytoplasm were picked up and cultured with 1000 μg/mL G418. Stably transfected SIRC cell lines were maintained in MEM supplemented with 10% FBS in the presence of G418 (1000 μg/mL).

A cell line that inducible expresses Pax6 protein designated as SP-10 (clone number 10), and one that inducible expresses truncated Pax6Δ286 protein, designated as SP-6 were used for further experi-

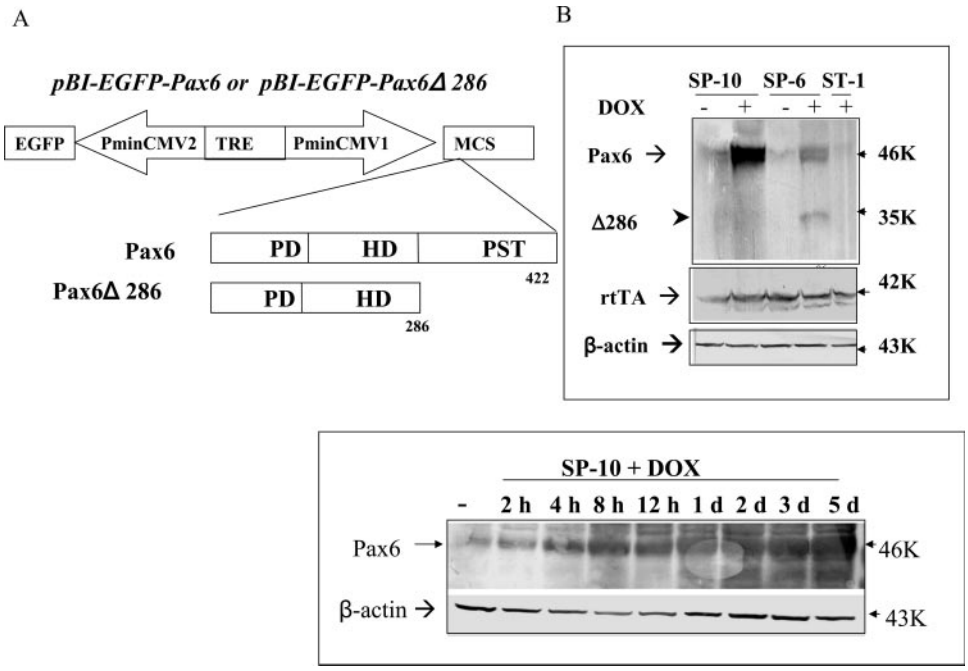

Figure 1. Schematic diagram of pBI-EGFP-Pax6 or pBI-EGFP-Pax6Δ286 and DOX-induction in transformed cell lines. (**A**) Relevant regions of the vector pBI-EGFP and the cDNA inserts used to generate the inducible cell lines. DOX binds the expressed protein rtTA, which then bind to the tetracycline-responsive element (TRE), driving bidirectional expression of EGFP and Pax6 or Pax6Δ286. (**B**) Cells were left untreated (−DOX), treated with 1 μg/mL DOX for 3 days (+DOX), or treated with 1 μg/mL DOX for the indicated hours or days. Western blot analysis prepared from lysates of cotreated SP-10, SP-6, and ST-1 cells were probed with antibodies against Pax6 to analyze for expression levels of Pax6 (SP-10 cell line) or the truncated form of Pax6, Pax6Δ286 (SP-6 cell line). The blots were then stripped and the expression level of the DOX-binding protein rtTA was similar probed. Molecular sizes are indicated based on the migration position of size standards run in a parallel lane. Reprobing for β-actin serves as a sample loading control. *Top*: a comparative analysis of cotreated cell lines. The antibody used was a monoclonal antibody against chick Pax6 amino acid 1-223 which recognizes both full-length and truncated Pax6. *Bottom*: a time course of treatment and withdrawal in the SP-10 cell line, using a polyclonal antibody generated against a peptide derived from the C-terminal of mouse Pax6 which recognizes only full-length Pax6.

ments (Fig. 1A). We also made a *pTet-On*-only transfected cell line as a control, designated as ST-1.

Construction of Recombinant Adenoviruses

The *mPax6* and *mPax6Δ286* fragments were excised from *pBI-EGFP-Pax6* and *pBI-EGFP-Pax6Δ286* plasmid, respectively, with *Bam*HI and inserted into the *pAdTrack-CMV* (http://www.coloncancer.org/adeasy.htm) to yield an adenoviral shuttle plasmid. The insert in the constructed plasmid was confirmed by DNA sequencing. Recombinant adenoviral plasmids were generated by homologous recombination in *Escherichia coli*, as described previously.[26] Purified viruses were aliquotted in 50% glycerol and stored at −20°C. The viral titer (PFU; plaque-forming unit, per milliliter) for adenovirus preparation was determined in 293 cells using 96-well plates and series-diluted virus for transfection. After 7 days, GFP expression was examined under an inverted fluorescence microscope to calibrate the viral titer.

Western Blot Analysis

Cultured cells were collected and solubilized in lysis buffer (250 mM NaCl, 50 mM Tris-Cl, 5 mM EDTA, 0.1% NP-40, 25 mM NaF, and protease inhibitor). After freeze-thawing and sonicating three times, total cell proteins were denatured by boiling 10 minutes with the equal volume of 2× Tris-glycine SDS sample buffer. Proteins in lysates were then separated by 4% to 20% SDS-PAGE, and transferred to polyvinylidene difluoride (PVDF) membrane. Two Pax6 antibodies were used to probe the blot: a monoclonal antibody against chick Pax6 amino acid 1-223 (developed by Atsushi Kawakami Developmental Studies Hybridoma Bank, University of Iowa, Iowa City, IA) and a polyclonal antibody generated against a peptide derived from the C-terminal of mouse Pax6 (Covance, Berkely, CA). The first antibody recognizes both full-length Pax6 and the truncated Pax6Δ286 protein, and was used when the product of the truncated Pax6Δ286 transgene was under analysis. The second antibody recognizes only full-length Pax6, but exhibited a stronger signal-to-noise ratio and so was used for all other experiments. Blots were also probed with rtTA antibody (VP-16 polyclonal antibody; BD-Clontech) and a monoclonal anti-β-actin antibody (Sigma-Aldrich).

Immunofluorescence Staining

Cells cultured in chamber slides were fixed with methanol for 10 minutes at room temperature and air-dried for 20 minutes. Primary antibodies were detected with a secondary antibody directed against the appropriate species labeled with Alexa Fluor 488 or 546 (Molecular Probes, Eugene, OR). The primary antibodies used were the same as those used in Western blots. Images were then captured (Axiocam MR5 imaging system; Carl Zeiss Meditec, Jena, Germany).

Cell Growth Curve and Population-Doubling Time

An equal number of cells (2×10^4) from the different stable cell lines *SP*-10, SP-6, and ST-1 were plated in triplicate in 100-mm dishes and cultured with or without DOX (1 ng/mL to 1 μg/mL). Cells were harvested at days 1, 3, 5, and 7 after plating. The total number of cells was counted in each individual plate with a hemocytometer, and the mean was calculated. The cell growth curve was drawn by plotting the mean cell number of each point against the culture time. Then, the *y*-axis of the growth curve was plotted using a log scale. The population-doubling time was estimated by the linear regression between log cell number and culture time.

MTT Cell Proliferation Assay

The 3-(4,5-dimethylthiazol-2-yl)-2,5-diphenyltetrazolium bromide (MTT) assay is based on the ability of a mitochondrial dehydrogenase enzyme from viable cells to cleave the tetrazolium rings of the pale yellow MTT and form dark blue formazan crystals. The crystals are largely impermeable to cell membranes, thus resulting in their accumulation within healthy cells. The number of surviving cells is directly proportional to the level of the formazan product created. Addition of a detergent results in the liberation of the crystals, which are solubilized along with cell membranes. The color is then quantified by reading on a multiwell scanning spectrophotometer (ELISA reader) at a wavelength of 570 nm, with the background subtraction at 650 nm. The amount of color produced, normalized against the background, is directly proportional to the number of viable cells and is represented as the relative proliferation index.

An equal number of cells (5×10^3) from the SP-10 or SP-6 transformed cell lines were seeded in each well of a 96-well plate and treated at a dose range of 1 to 1000 ng/mL of DOX for 3 days. Each treatment was repeated 8 times. The MTT cell proliferation assay was performed according the manufacturer's instructions (Promega, Madison, WI). The mean proliferation index for each treatment was analyzed for statistical significance using ANOVA if more than two groups were compared, or by two-tailed unpaired Student's *t*-test if only two groups.

Apoptosis Assays

The TUNEL assay was performed to detect apoptotic cells. Briefly, cells of the SP-10 cell line were separated and cultured with or without 1 μg/mL DOX in chamber slides for 3 days. The TUNEL assay was performed according to the manufacturer's instructions (Promega). Images were viewed and captured (Axiocam MR5; Carl Zeiss Meditec). The apoptotic cells were counted in five fields and compared by two-tailed unpaired *t*-tests between each two groups. Caspase-3 activity was compared (caspACE, colorimetric assay system; Promega), that provides a colorimetric substrate and a cell-permeable pan-caspase inhibitor (Z-VAD-FMK) that allow highly sensitive, quantitative measurement of caspase-3 activity. Western blot analysis, as described earlier was also used to detect the Bax and caspase-3 and -9 protein levels in the SP-10 cell line, with or without DOX treatment. The primary antibodies used were Bax, caspase-3, and caspase-9 (all from Santa Cruz Biotechnology, Santa Cruz, CA).

Cell Cycle Kinetics Analysis

Cells (2×10^5) were plated in 100-mm dishes and cultured in medium with or without 1 μg/mL DOX. Nocodazole (0.3 μg/mL; Sigma-Aldrich) was added into culture medium to block cell cycle progression at the M phase. The cells were harvested at 0, 8, 16, 24, and 48 hours after nocodazole treatment, washed twice in salt buffer (1% BSA and 0.5% sodium azide in PBS), and fixed by 70% ethanol at 4°C overnight. After they were washed twice in salt buffer again, the cells were stained in propidium iodide (PI) solution 50 μg/mL (Sigma-Aldrich) containing RNase 100 μg/mL for 1 hour. Then, they were transferred to flow cytometry tubes with filter for cell cycle analysis.

BrdU Pulse–Chase Labeling

Cells of the SP-10 transformed cell line were plated in chambered slides over night. A subset of the cultures was treated with 1000 ng/mL DOX. The next day, 20 μM bromodeoxyuridine (BrdU; Roche, Indianapolis, IN) was added to the medium for 2 hours. During this "pulse" most of the cells incorporated BrdU into their DNA as they entered the S-phase of the cell cycle. Cells were then washed with PBS three times and incubated in medium, with or without 1000 ng/mL DOX for 3 days. After this chase, the cells were fixed for 15 minutes with 4% paraformaldehyde in PBS, treated with 2 M HCl for 1 hour at 37°C, and stained with mouse anti-BrdU antibodies (Neomarker, Fremont, CA) in 0.5% Triton X-100 and 1% BSA in PBS for 2 hours at room temperature. After they were washed twice, the cells were further incubated with FITC-conjugated goat anti-mouse IgG (Molecular Probes) in 1% BSA in PBS for 1 hour at room temperature. Images were viewed and captured (Axiocam MR5; Carl Zeiss Meditec, Inc.) all with the same exposure time. Photographs were taken from five fields with the similar cell number in each slide and the mean fluorescence intensity of the fields was calculated (Adobe Systems Inc., San Jose, CA). The fluorescence intensity was normalized using the SP-10 cells without DOX treatment after 2 hours of BrdU labeling as the control.

RESULTS

DOX-Dependent Expression of *Pax6* or Truncated *Pax6* and Location of Proteins

Western blot analysis was performed to compare DOX inducibility of the transgenes in the SP-10 cell line carrying the full-length *Pax6* construct, the SP-6 cell line carrying the truncated Pax6Δ286 construct, and the ST-1 control cell line carrying the empty vector. Representative results are shown in Figure 1B. In the absence of DOX, a small amount of a 46-kDa protein immunoreactive with Pax6 antibody was present in all three transformed cell lines, appropriate in size to be full-length Pax6 (Fig. 1B, top). This was most likely expressed from the endogenous *Pax6* gene, since it was not dependent on the presence of a *Pax6* cDNA insert in the transgene (untreated line SP-6 and DOX-induced control line ST-1 showed similar levels as untreated line SP-10).

DOX treatment of SP-10 cells resulted in a dramatic increase in the level of this 46-kDa protein in the SP-10 cell line, consistent with induced expression of the full-length *Pax6* transgene (Fig. 1B, top). This increase began within 4 hours after the addition of DOX and attained a plateau within 2 days (Fig. 1B, bottom). DOX treatment of SP-6 cells resulted in the appearance of a new Pax6 immunoreactive protein which ran at 35 kDa, appropriate in size to be the product of the truncated *Pax6* transgene and consistent with its induced expression (Fig. 1B, top). Immunofluorescence analysis using a polyclonal antibody generated against a peptide derived from the C-terminal of mouse Pax6 revealed that DOX-induced Pax6 was sequestered in cell nuclei, indicating that it was available for transcriptional activation (Supplementary Fig. S1, available online at http://www.iovs.org/cgi/content/full/47/6/2397/DC1). This experiment also showed that the expression of green fluorescent protein (EGFP) was also dependent on DOX and functioned as a surrogate marker of Pax6 expression (Supplementary Fig. S1). EGFP and Pax6 levels were both returned close to original levels after DOX was removed from the culture media (Supplementary Fig. S1). These results indicate that the DOX-inducible system was fully functional and that expression of the transgenes in the transformed cell lines was dependent on the presence of DOX.

Other changes in the levels of Pax6 immunoreactive proteins also occurred after DOX treatment that were not so readily explained. A very small amount of a lower-molecular-weight band also became visible as the levels of Pax6 became highly elevated in DOX-treated SP-10 cells (Fig. 1B, bottom). This protein was larger than the product of the truncated *Pax6* transgene and could not be visualized with the antibody to the amino terminal of Pax6 (Fig. 1B, top). This may represent a degradation product of Pax6 that could be present endogenously, but may also be an artifact generated during the process of lysate preparation. This protein may well be present in uninduced cells at the same ratio with respect to full-length Pax6, but it may be undetectable on the Western blot, because its level is so low. However, because it represents such a small part of the total Pax6-immunoreactive protein, it seems unlikely that it would contribute significantly to any changes in cell phenotype due to full-length Pax6 overexpression.

A more significant change in the ratio between Pax6 and truncated Pax6 occurred in the DOX-induced SP-6 cell line in response. In addition to induction of the truncated Pax6 transgene, a small but clear increase in the full-length 46 kDa immunoreactive protein occurred in DOX-treated SP-6 cells. This increase seemed to be dependent on expression of the truncated Pax6 protein as the level in the DOX-treated ST-1 control cell line was the same as the uninduced levels in the SP-10 and SP-6 cell lines. Visual inspection of the band intensity on the Western blot suggested that the level of endogenous Pax6 and the level of truncated Pax6 are roughly equivalent (taking into account that the upper Pax6 immunoreactive band is darker, but that the protein is also larger). It is possible that this secondary induction is due to a feedback loop. Whatever the reason, it is important to take under consideration in drawing conclusions from the data presented in the following sections.

Effect of Overexpression of Pax6 on Cell Proliferation

To determine whether Pax6 overexpression affects cell proliferation, we compared the cell growth curve in lines SP-10 and SP-6, with or without DOX treatment. As shown in Figure 2, top right, the population-doubling time for SP-10 cells in the absence of DOX was 12 hours, but was prolonged to 16, 20, and 40 hours in the presence of 10, 100, and 1000 ng/mL DOX, respectively (Fig. 2, top). After 5 days of DOX removal from culture media, the cell growth curve and population-doubling time almost returned to normal. DOX itself had no inhibitory effect on the proliferative index, as evidenced by the fact that the population-doubling time remained 12 hours, even when cells of the ST-1 control cell line were cultured in 1000 ng/mL DOX. In contrast, DOX treatment of SP-6 cells harboring truncated Pax6 had no effect on the cell growth curve and population-doubling time (Fig. 2, top right).

We used the MTT assay as a second way to measure cell proliferation. Induction of Pax6 expression by treatment of SP-10 cells with DOX decreased the proliferative index in a dose-dependent manner (Fig. 2, lower left). This was reversed when DOX was removed from the culture medium for 5 days (Fig. 2, bottom middle). In contrast, DOX-treatment of SP-6 cells did not change the proliferative index (Fig. 2, bottom right). As determined by Western blot analysis, the proliferative index was directly correlated with the full-length Pax6 expression level in SP-10 cells, but not with the level of truncated Pax6 in SP-6 cells (data not shown).

Taken together, these results show that elevation of Pax6 inhibits cell proliferation in a dose-dependent manner and that this effect is fully reversible. In contrast, increasing the levels of Pax6 along with truncated Pax6 by DOX treatment in the SP-6 cell line has no effect on cell proliferation. This is consistent with a dominant-negative activity for truncated Pax6 and suggests that the transcriptional transactivation domain is necessary for an effect on the cell proliferation rate.

Effect of Overexpression of Pax6 on the Cell Cycle Profile

Both proliferation assays measured the total number of cells in the sample over a time course. Thus, the reduction in the cell proliferation rate could be due to slower progression of individual cells through the cell cycle or to increased cell death. To distinguish between these two possibilities, we compared the cell cycle profile in cell lines SP-10 and SP-6, with or without DOX treatment. Cells were treated with PI to stain DNA then sorted for PI levels by flow cytometry, generating a profile of the cell population indicative of their cell cycle stage. We found that the percentage of cells in both G_0/G_1 and sub-G_1 increased with Pax6 overexpression in the SP-10 cells (Fig. 3). Analysis of the cell cycle by flow cytometry showed that after 3 days of culture in the presence of DOX, 63% of the cells were in G_0/G_1, whereas 58% of the untreated cells were in G_0/G_1 (Fig. 3). After 3 days of DOX induction (1 μg/mL), the proportion of sub-G_1 phase cells increased to 8% compared with 4% of SP-10 cells without DOX (Fig. 3). The sub-G_1 peak comprises cells containing less than 1 N chromosomal copy, including apoptotic cells undergoing chromosomal degradation. These

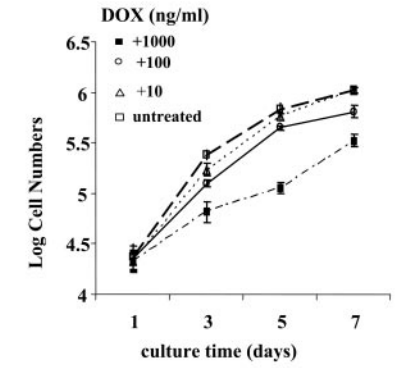

Cell line	DOX dose	Treatment	Doubling Time
SP-10	untreated	Continuous	12 hours
SP-10	1ng/ml	Continuous	12 hours
SP-10	10ng/ml	Continuous	16 hours
SP-10	100ng/ml	Continuous	20 hours
SP-10	1000ng/ml	Continuous	40 hours
SP-10	1000ng/ml	3 day only	12 hours
ST-1	untreated	Continuous	12 hours
ST-1	1000ng/ml	Continuous	12 hours
SP-6	untreated	Continuous	12 hours
SP-6	10ng/ml	Continuous	12 hours
SP-6	100ng/ml	Continuous	12 hours
SP-6	1000ng/ml	Continuous	12 hours

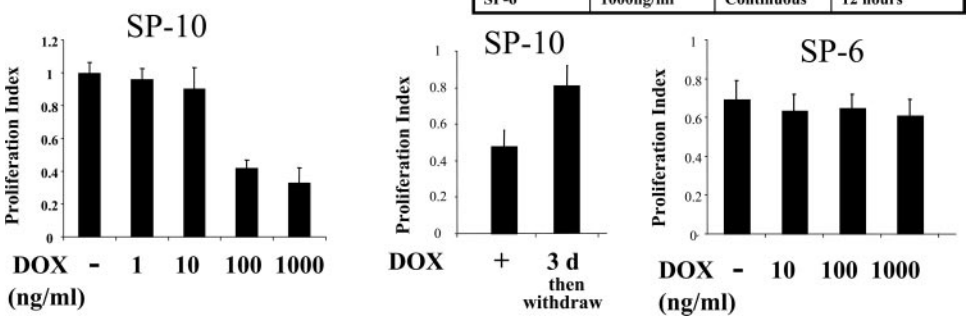

FIGURE 2. Cell proliferation analysis after induction of Pax6 or truncated Pax6 in SP-10 or SP-6 cell lines. *Top*: Proliferation assay. *Left*: log growth curve for SP-10 cell cultures in which Pax6 expression was induced with increasing concentrations of DOX. Three independent determinations were made for each time point, with SEM. The *x*-axis is the relative proliferation index presented by the value obtained from the colorimetric assay. *Right*: calculated population-doubling times for the dose–response, and after treatment for 3 days with DOX followed by drug withdrawal. The ST-1 cell lines serves as a control for the nonspecific effects of DOX. *Bottom*: MTT assay. *Left*: calculated proliferation index for SP-10 cell cultures in which Pax6 expression was induced by treatment with DOX for 3 days with increasing concentrations of DOX; untreated (−DOX) and 1, 10, 100, and 1000 ng/mL ($P < 0.0001$ by ANOVA; $n = 8$). *Middle*: calculated proliferation index for SP-10 cell cultures; Pax6 expression was induced by continuous treatment with DOX (+DOX) or after DOX treatment for 3 days followed by withdrawal for 5 days (3 d then withdraw) ($P < 0.05$ by two tail unpaired *t*-test; $n = 8$). *Right*: calculated proliferation index for SP-6 cell cultures in which truncated Pax6 (Pax6Δ286) expression was induced by treatment with DOX for 3 days with increasing concentrations of DOX; untreated (−DOX) and 10, 100, and 1000 ng/mL ($P = 0.07$ by ANOVA, $n = 8$). Relative proliferation index is directly proportional to the number of variable cells in the samples.

data suggest that some part of the decrease in cell proliferation after DOX treatment of SP-10 cells may be due to apoptotic cell dropout.

We quantified the inhibition of cell cycle progression in DOX-treated SP-10 cells by comparing the time it takes for the cell population to be synchronized at M phase in untreated and DOX-treated cells. Cultures were left untreated or treated overnight with DOX to induce Pax6 to high levels. Then, both groups were further treated with nocodazol, a drug that blocks cell cycle progression at the G_2/M transition by depolymerization of the microtubules needed for mitosis. The cultures were sampled at progressing time points thereafter, and analyzed by staining with PI and sorting for DNA content. Before nocodazole treatment, the cell cycle profile looked similar in both groups. In the first 8 hours, there was no difference between SP-10 cells, with or without DOX induction. However by 16 hours after adding nocodazol, there was a dramatic difference between these two groups. Whereas 52.1% of the control SP-10 cells were blocked in the G_2/M phase, only 33.6% of the DOX-induced SP-10 cells had reached the G_2/M phase. The difference was even more dramatic if we compared the cell cycle profile 24 hours after adding nocodazole. At this time, 66.5% of the SP-10 cells without DOX addition cells were in the G_2/M phase, but only 37.2% of cells with DOX induction were in the G_2/M phase (Fig. 4A). When cells were incubated with nocodazole in the presence of DOX up to 48 hours, additional cells (15.7%) entered G_2/M phase (Fig. 4A). Approximately 28% of SP-10 cells overexpressing Pax6 entered G_2/M phase in 8 hours (after adding nocodazole from 8 to 16 hours), and 28% entered the G_2/M phase in 40 hours (after adding nocodazole from 8 to 48 hours). The continued higher frequency of 2 N nuclei (G_0/G_1) in the DOX-treated group at the 48-hour time point (26.3% in +DOX versus 8.3% in untreated) suggests that there were still more cells that had either arrested in G_1 or dropped out of the cycle.

This phenomenon of retarded progression of the cell population through the cell cycle in DOX-treated SP-10 cells overexpressing full-length Pax6 did not occur in cells of the SP-6 line overexpressing truncated Pax6 (Fig. 4B).

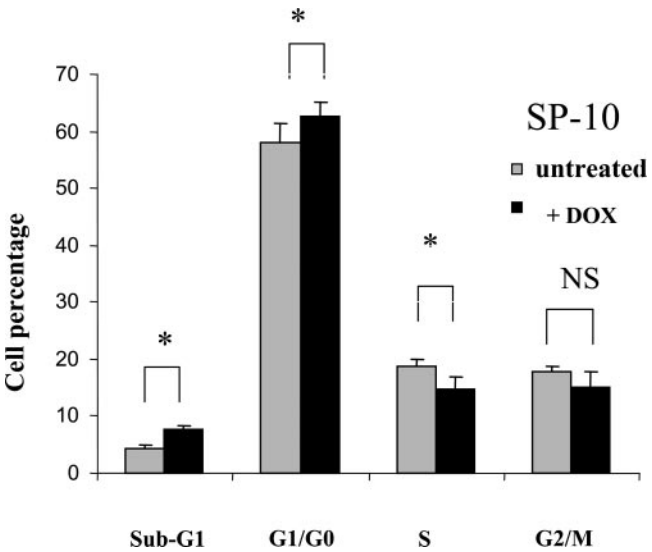

FIGURE 3. Cell cycle profile after induction of Pax6 in the SP-10 cell line. Cell cycle profiles were generated by flow cytometry of PI-stained cells, and the percentage of cells in the PI peaks (representing different DNA content) was graphed. Cells were left untreated, or treated with DOX at 1 μg/mL to induce expression of Pax6 for 3 days in SP-10 cells. Cell samples were stained with PI and cell cycle profile was determined by flow cytometry. The percentage of the cell population in each cell cycle phase is indicated on the *y*-axis. *Significance at the level of $P < 0.05$ by the two-tailed unpaired *t*-test, $n = 5$. NS, no significance at the level of $P < 0.05$ by two-tailed unpaired *t*-test, $n = 5$.

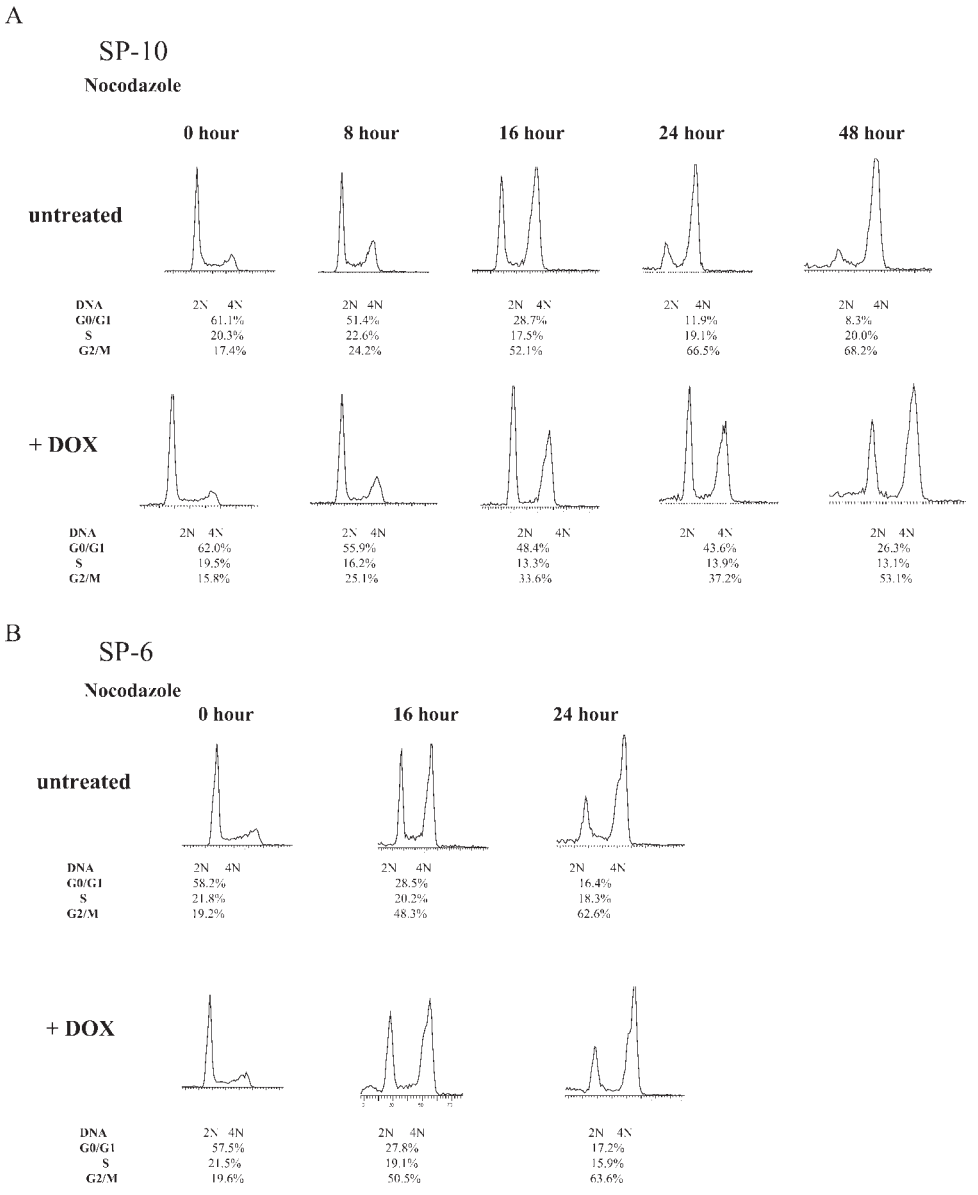

FIGURE 4. Cell cycle kinetics analysis after induction of Pax6 or truncated Pax6 in the SP-10 or SP-6 cell lines. Cells were left untreated or treated with DOX at 1 μg/mL overnight to induce expression of Pax6 in SP-10 cells or truncated Pax6 (Pax6Δ286) in SP-6 cells. The next day, nocodazole at 300 ng/mL was added to block mitosis. To follow the transit of cells from G_0/G_1 to G_2/M, cell samples were stained with PI at select time points up to 48 hours, and the cell cycle profile was determined by flow cytometry. The percentage of the cell population in each cell cycle phase is indicated below each profile; (**A**) SP-10 cells; (**B**) SP-6 cells; 2N, G_0/G_1; 4N, G_2/M.

Effect of Overexpression of Pax6 on Individual Cell Progress through the Cell Cycle

To investigate whether individual cells in the DOX-treated SP-10 cell population overexpressing Pax6 were retarded from progressing through the cell cycle, we performed a BrdU pulse–chase labeling experiment (Fig. 5). SP-10 cells treated with DOX incorporated 20% less BrdU than untreated cells in a 2-hour pulse. After 3 days of chase, there was a decrease in the total BrdU-fluorescence intensity of selected microscopic fields containing a similar number of cells in both the untreated and DOX-treated groups (Fig. 5, bottom). This indicated that DNA replication and cell division had occurred, diluting the amount of labeled DNA. However, the reduction in fluorescence intensity was considerably less in the DOX-treated cells than in the untreated cells. The reduction in fluorescence intensity appeared very similar between individual cells in each field, and the same percentage of cells contained label before and after the chase, which indicated that the overall reduction in fluorescence intensity of the microscopic fields was not due to the behavior of a select portion of the population. This result provides evidence that overexpression of Pax6 retards progress of the cell population through the cell cycle by causing slow cycling of individual cells.

Effect of Overexpression of Pax6 on Caspase-Independent Apoptosis in a Small Percentage of Cells

The proportion of cells in the sub-G_1 phase increased to 14% in SP-10 induced with DOX after 5 days of culture (Fig. 6, top). But the percentage of sub-G_1 cells in the SP-6 cell line, and ST-1 control cell lines remained lower than 5%, even after 5 days in the presence of DOX (Fig. 6, top).

Cells in the sub-G_1 phase of the flow cytometry profile contain less DNA than cells in G_1, consistent with apoptosis. To provide further evidence of an increase in apoptosis in Pax6 overexpressing cells, a TUNEL assay was performed on SP-10 cells with DOX induction. The results were consistent with the flow cytometry data. The number of apoptotic cells increased with Pax6 overexpression (Fig. 6, bottom). We used the pan-caspase inhibitor (Z-VAD-FMK; Promega) to determine whether induction of apoptosis by Pax6 overexpression is caspase dependent. After incubation in culture media with 50

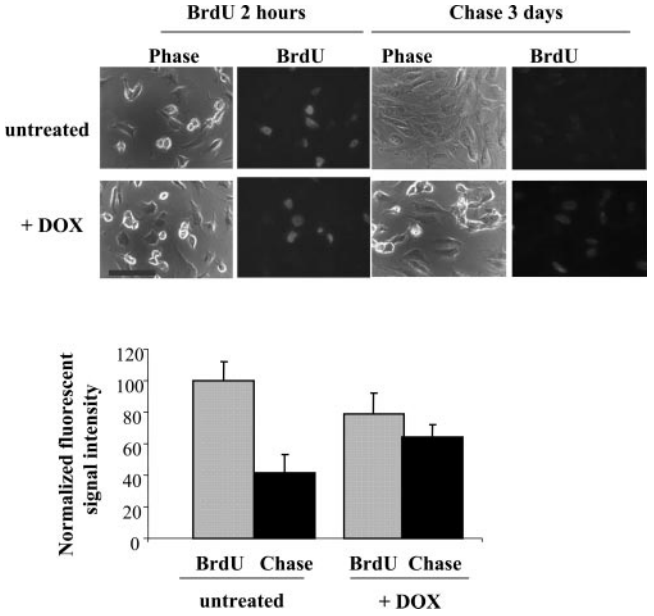

FIGURE 5. BrdU pulse chase labeling after induction of Pax6 in the SP-10 cell line. Cells of the SP-10 cell line were left untreated or treated with DOX at 1 μg/mL overnight to induce Pax6 expression. The next day, BrdU was added for 2 hours. During this "pulse" most of the cells incorporated BrdU into their DNA as they entered the S-phase of the cell cycle. Cells were then washed and left untreated or further treated with DOX for 3 days. After this "chase," the cells were fixed, and BrdU was localized within cells by indirect immunofluorescence, using a rhodamine-conjugated secondary antibody. *Top*: cells were viewed by phase-contrast (phase) or fluorescence microscopy using appropriate filters (BrdU). *Bottom*: the mean fluorescence intensity of BrdU staining was quantified.

μM Z-VAD-FMK for 16 hours, SP-10 cells were induced with DOX for 3 days. There was no evidence of a decrease in the number of apoptotic cells (Fig. 6, bottom). Backing up this conclusion, the caspase-3 activity as detected by an assay (CaspACE Assay System; Promega) had no difference in SP-10 cells, with or without DOX treatment (data not shown). Also, the Bax, caspase-3, and caspase-9 expression levels and cleavage products as detected by immunoblot analysis showed no difference in SP-10 cells, with or without DOX treatment (data not shown).

Effect of Transient Overexpression of Pax6 on Cell Proliferation in Primary Cultures of Corneal Epithelial Cells

SIRC cells are derived from corneal epithelium and retain many of the features of this cell type. However, they have also lost many of these features, including cornea-specific keratin expression. Also of concern is the fact that SIRCs are an immortalized cell line, indicating that genes affecting cell proliferation and lifespan have been altered. To enable us to confirm our results in freshly isolated primary rabbit epithelial cells (RCECs) in culture, we constructed recombinant adenovirus vectors carrying *mPax6* or *mPax6Δ286* gene to enable transduction (Fig. 7). A difficulty with this method is that it results in a mixed population of transduced and nontransduced cells. To overcome this drawback, we sought to achieve a high percentage of transduction by using a high adenovirus concentration (50 PFU/cell). This method was successful, as more than 95% of the RCECs were transduced, as assessed by EGFP fluorescence (Fig. 7, top right). The expression of the Pax6 and Pax6Δ286 proteins was confirmed by Western blot (Fig. 7, top left) and immunostaining (Fig. 7, top right). Endogenous Pax6 was not detectable in this experiment, and there was no evidence for its upregulation by *mPax6Δ286*, unlike in the SIRC cells. After 2 days of transduction, the cells were collected and stained with PI to study the cell cycle profile by using flow cytometry. The percentage of cells in the G_0/G_1 phase increased more than 10%, whereas the percentage in the S-phase was reduced approximately 10% in Pax6-overexpressing cells (Fig. 7, bottom). The percentage of G_2/M phase cells

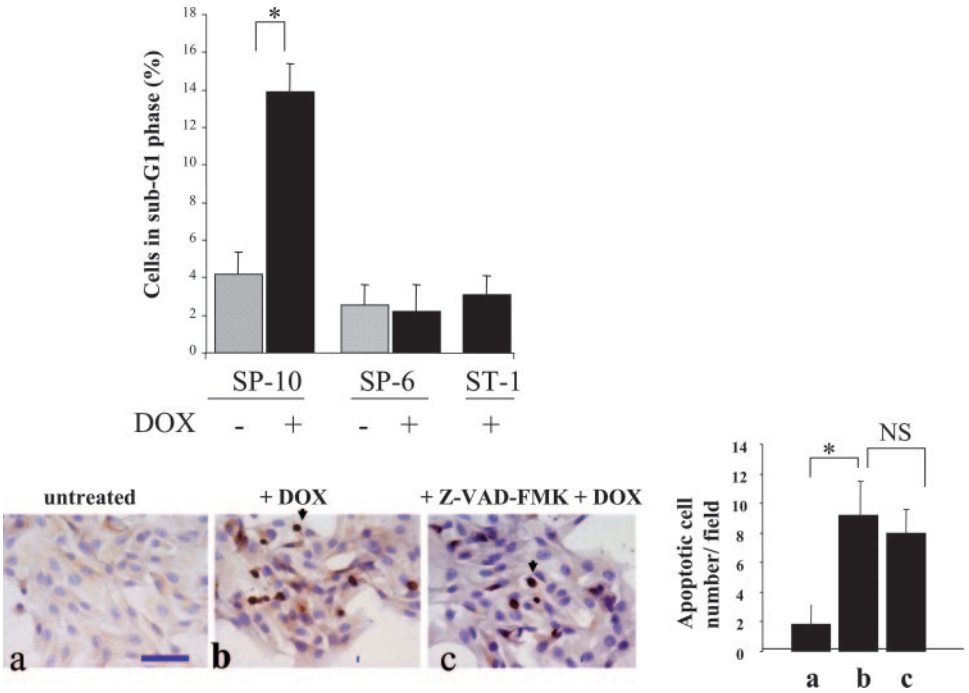

FIGURE 6. Apoptosis analysis after induction of Pax6 or truncated Pax6 in the SP-10 cell line. *Top*: cell cycle profiles were generated by flow cytometry of PI-stained (PI) cells, and the percentage of cells in the sub-G_1 phase (representing DNA content <2 N) was graphed. Cells were left untreated (▨) or were treated with DOX at 1 μg/mL (■) to induce expression of Pax6 (SP-10 cell line) or truncated Pax6 (SP-6 cell line) for 5 days. ST-1 expressed rtTA only as a control of the DOX effect. *Significance at the level of $P < 0.05$ by the two-tailed unpaired *t*-test, $n = 5$. *Bottom left*: TUNEL assay comparing untreated SP-10 cells, SP-10 cells treated with DOX for 3 days, and SP-10 cells treated with DOX plus the pan-caspase inhibitor Z-VAD-FMK at 50 μM. *Arrow*: apoptotic nucleus stained *deep brown*. There is no evident inhibitory effect on the number of apoptotic cells by Z-VAD-FMK pretreatment. *Bottom right*: data obtained from the experiment depicted at *left* were quantified. *Significance at the level of $P < 0.05$ by the two-tailed unpaired *t*-test, $n = 5$. NS indicates that there was no significance at the level of $P < 0.05$ by the two-tailed unpaired *t*-test, $n = 5$.

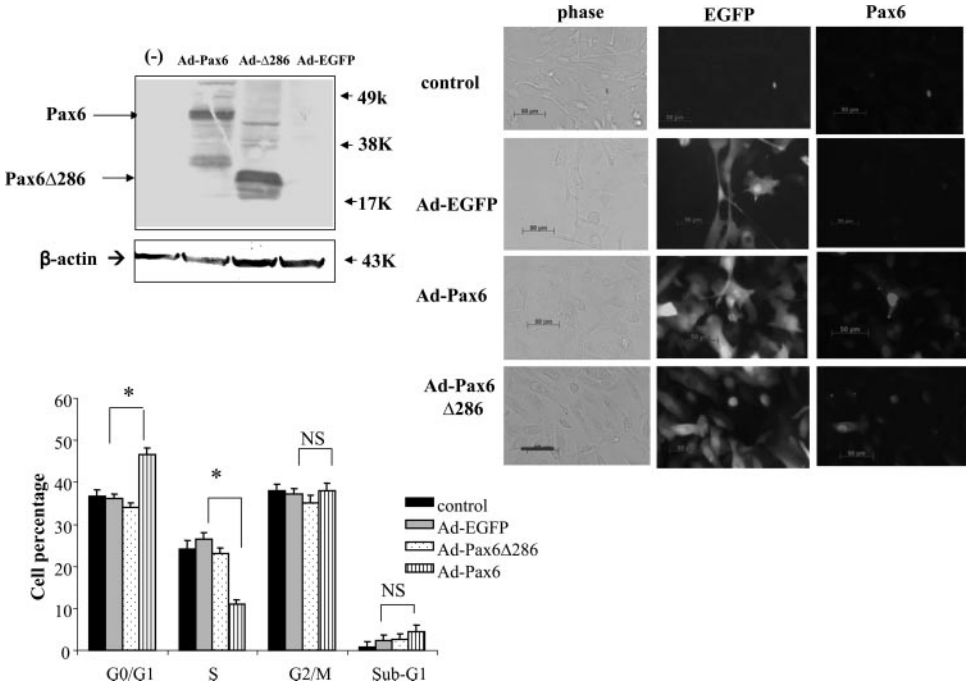

FIGURE 7. Effects of transient overexpression of Pax6 or truncated Pax6 in primary rabbit corneal epithelium cells (RCECs). RCECs were infected at high efficiency with adenoviral vectors carrying Pax6 (Ad-Pax6), truncated Pax6 (Ad-Pax6Δ286), or empty vector expressing EGFP only (Ad-EGFP). *Top left*: Western blot analysis prepared from lysates of noninfected cells (−) or cells with the vectors probed with a monoclonal antibody against chick Pax6 amino acid 1-223 which recognizes both full-length and truncated Pax6, to analyze for expression levels of the inserts. Molecular sizes are indicated based on the migration position of size standards run in a parallel lane. Reprobing for β-actin served as a sample loading control. The lower band in the Ad-Pax6 lane probably represents a degradation product. The identity of the *top* band in the Ad-Δ286 lane is unknown, but because it is a minor in comparison to the Pax6Δ286 band, it probably would not affect the results. *Top right*: cells were transduced with the adenoviral vectors (50 PFU/cell) for 2 days. Indirect immunofluorescent localization of expressed Pax6 protein was performed using a monoclonal antibody against chick Pax6 amino acid 1-223, which recognizes both full-length and truncated Pax6 as a primary antibody. A rhodamine-conjugated secondary antibody was used to visualize binding, and cells were viewed by phase contrast (phase) or fluorescence microscopy using appropriate filters (EGFP or Pax6). Bar, 50 μm. *Bottom*: cell cycle profiles were generated as in Figure 5 in cells transduced with adenoviral vectors to compare the effects of Pax6 or truncated Pax6-expressing cells. The percentage of cells in the different phases was graphed. *Significance at the level of $P < 0.05$ by two tailed unpaired *t*-test; $n = 3$. NS indicates that there was no significance at the level of $P < 0.05$ by the two tail unpaired *t*-test; $n = 3$.

remained unchanged. This change was not evident in the *mPax6Δ286* transfected cells. These results indicate that transient overexpression of full-length Pax6 also alters the cell cycle profile in primary corneal epithelial cell cultures.

DISCUSSION

In this study, we investigated the role of *Pax6* in modulating corneal epithelial cell dynamics by overexpressing it in an inducible cell culture model. We made some novel findings that provide insight into mechanism and biological significance.

Direct Inhibition of Proliferation of Corneal Epithelial Cells

Several in vivo studies have suggested that Pax6 affects cell proliferation. The direction of the effect, however, appears to be tissue and context dependent. For example, telencephalic neurons proliferate more rapidly in SEY heterozygotes than in wild-type littermates, whereas diencephalic neurons proliferate more slowly.[27–29] Corneal epithelial cell proliferation is increased 10-fold over normal in SEY heterozygote mice.[22] SEY heterozygote lenses are smaller because a deficiency of Pax6 results in one or two fewer rounds of cell division during early lens development.[30] In contrast, Pax6 expression in the lens is highest in the replicative epithelial cells, but is downregulated in the fiber cells, which withdraw from the cell cycle.[31] Adult corneal epithelium, isolated and recombined with embryonic dermis, transdifferentiates into epidermis through a progression of steps; this includes downregulation of Pax6, which is accompanied by an increase in the epithelial cell proliferative rate.[32] In all these studies, Pax6 effects could be either direct or indirect. For example, in the corneal SEY study it was unclear whether the increased proliferative index in the epithelium was directly due to Pax6 deficiency or was the indirect result of cell loss from the upper layers due to perturbed cell adhesions.[22] Also of importance is a consideration of developmental factors. Epithelial stem cell deficiency due to a reduction in Pax6 may alter the composition of the epithelium.

Our study used a simplified model of cultured rabbit corneal epithelial cells to avoid the confounding factors of a complex system. We chose to use the DOX-inducible system to allow tight control over the levels of Pax6. When we induced high levels of Pax6 by DOX treatment, cell proliferation was inhibited in stably transformed cells of the SIRC line. This effect was reproducible in primary rabbit corneal epithelial cells (RCECs) transduced by recombinant *Pax6* adenovirus. The findings are consistent with those of another recent cell culture study that showed that overexpression of Pax6 in corneal epithelial cells attenuates EGF-induced cell proliferation, whereas knockdown of Pax6 mRNA levels with small interfering RNA promotes EGF-induced cell proliferation.[33] Our study provides new insight, however; we further demonstrated that the effect could be completely reversed by returning Pax6 levels to normal through withdrawal of DOX. These results support a direct role of Pax6 in the regulation of cell proliferation.

Effect of Elevation of Pax6 Levels

Flow cytometry showed that cell cycle progression was retarded in Pax6-overexpressing cells. Further analysis using the M-phase blocker, nocodazole, showed that Pax6 overexpressing cells—as a population—took a much longer time to reach the G_2/M phase. The BrdU experiment provided evidence that slow cycling was a property of individual Pax6 overexpressing cells. In addition to inhibition of cell cycle progression, overexpression of Pax6 led to apoptosis in a small percentage of cells. These findings are consistent with those of a study investigating the role of *Pax6* in cell proliferation in a neuroblas-

toma cell line.[34] No changes in cell-doubling time were observed in cell lines stably transformed with Pax6. However, this could be due to selection of transformed cells with secondary changes that allowed them to expand into identifiable colonies, a confounding factor that was avoided by our use in an inducible system in this study. Transient overexpression of Pax6 via an adenoviral vector in the neuroblastoma cells, however, suppressed cell growth by increasing the number of cells in G_1 and by decreasing the number of cells in the S-phase.[34] Later on, it also caused cell death.

Evidence That *Pax6* Effects Are Due to Transcriptional Activity

Another novel contribution of this study was evidence that the *Pax6* effects are mediated by transcription. We demonstrated that overexpressed Pax6 was sequestered in the nucleus of cells, where it would be available to bind to gene transcriptional promoters (Supplementary Fig. S1, http://www.iovs.org/cgi/content/full/47/6/2397/DC1). Overexpression of the truncated *Pax6Δ286*, which lacks the transcriptional activation domain, showed none of the effects of the full-length Pax6 in either SIRC cells or RCECs. In fact, we found that endogenous Pax6 levels were also obtained with induction of truncated Pax6 at roughly an equivalent level. That induction of full-length Pax6 in the presence of truncated Pax6 had no effect on cell dynamics is consistent with the previously described dominant-negative activity of truncated Pax6.[25] This suggests that the Pax6 transcriptional activation domain is the key and supports the concept that Pax6 exerts its effect on cell dynamics by altering transcription of genes involved in cell cycle progression and apoptosis in corneal epithelial cells.

To orchestrate the complex events of eye development, transcription factor Pax6 must ultimately control activity of a large number of downstream genes. It can do this both directly and indirectly. For example, Pax6 directly controls the promoters for keratin 12 (*K12*),[35,36] and the alpha4 integrin subunit in corneal epithelial cells.[37] Pax6 also controls expression of matrix metalloproteinase gelatinase B (MMP9), induced at the migrating epithelial wound front.[38,39] It activates the MMP9 promoter by binding DNA directly or by binding indirectly via AP-2α transcription factor,[38,39] which is also upregulated at the migrating corneal epithelial wound front.[40] AP-2α regulates N-cadherin expression in corneal epithelial cells,[41] and its deficiency has effects on eye development similar to those of Pax6 deficiency.[42,43]

The genes that Pax6 regulates to inhibit the cell cycle remain to be identified. MMP9 inhibits the rate of corneal epithelial cell proliferation in vivo.[40] However, in this study, we found no apparent change in MMP9 expression in Pax6-overexpressing SIRC cells (data not shown). In lens cells, Pax6 was shown to interact with retinoblastoma (RB) protein, a transcription factor that controls cell cycle progression.[25] However, in this study, we were unable to demonstrate an interaction between Pax6 and RB (data not shown). A cDNA microarray analysis comparing SEY heterozygotes with their normal counterparts revealed a spectrum of genes regulated by Pax6 in mouse lens, including four genes involved in cell growth, division, and DNA synthesis.[44] A similar microarray analysis on the Pax6-overexpressing SIRC cell lines created in our study may help to answer the question of Pax6 targets in this situation.

Biological Significance

Pax6 overexpression in SIRC cells slowed down cell cycle progression, but did not completely arrest it, as forward progress could be seen in the BrdU experiment. BrdU was retained longer by the Pax6-overexpressing cell line than by the noninduced cells, but was gradually lost. Prolonged BrdU label retention is a hallmark of stem cells, which are very slow cycling.[7] In the developing retina, Pax6 expression is essential for the multipotency of retinal precursor cells, as the absence of Pax6 leads to the presence of only amacrine cells.[44] Pax6 has been identified as a marker of corneal stromal stem cells.[45] One of the consequences of reduced Pax6 dosage in humans or SEY mice is corneal epithelial stem cell deficiency.[46,47] This suggests a possible biological role for Pax6 in maintaining stem cells.

Another possibility is corneal re-epithelialization after injury. We previously demonstrated that Pax6 protein levels and DNA-binding activity are elevated at the front of epithelial cells migrating to close a wound.[48] Cell migration and cell proliferation are often seen to be mutually exclusive, and cell proliferation in repairing corneal epithelium takes place primarily in the region behind the migrating front.[40] Our results suggest that upregulation of *Pax6* levels may be involved in retarding cell proliferation at the epithelial wound front.

The lens represents an intriguing model for understanding how *Pax6* may regulate both cell cycle withdrawal and apoptosis. As discussed, Pax6 is expressed in high levels in the replicative epithelial cells surfacing the lens capsule, but is downregulated once these migrate around the bow region and differentiate into fiber cells.[31] Lens fiber cells represent an interesting intermediate between cell cycle quiescence and apoptosis, as they lose their nuclei but continue to remain alive. In a TGF-β-induced model of pathologic subcapsular cataract, lens epithelial cell transformation into replicating myofibroblasts is associated with a downregulation of *Pax6*.[49] It was noted that in lenses of SEY mice anterior subcapsular plaques also spontaneously develop. These results suggest that a reduction in *Pax6* levels may be essential for this pathologic process to progress.

Although Pax6 protein is present in most cells of the central and peripheral epithelium, it is reduced or absent in the most superficial cellular layer of the corneal epithelium,[22] where the flattened cells are released from the surface of the multilayer in a process known as "desquamation." Results in studies have suggested that desquamating cells are apoptotic.[50] In a culture system developed to mimic the native corneal epithelial sheet, electron microscopy showed cells in various morphologic states of desquamation.[51] Surprisingly, few of these cells showed evidence of apoptosis, either by morphologic or DNA fragmentation analyses. These results suggest a new model for desquamation from stratified epithelia, in which desquamation and apoptosis are independent and sequential processes. It will be fascinating to examine the relationship between Pax6 expression and the process of desquamation by using this model.

The cell death that occurred in the small percentage of cells overexpressing Pax6 in this study was characterized as apoptotic by TUNEL assay, but was caspase independent. Patterns of cell death have been divided into apoptosis, which is actively executed by the caspases, and accidental necrosis. However, there is now accumulating evidence indicating that cell death can occur in a programmed fashion but in complete absence and independent of caspase activation.[52] Caspase-independent cell death pathways are important safeguard mechanisms to protect the organism against unwanted and potentially harmful cells when caspase-mediated routes fail. The biological significance in our situation is not known; however, the possible connection to the process of desquamation will be interesting to explore.

Conclusions and Future Directions

The current data are consistent with the notion that Pax6 acts to "put the brakes on" corneal epithelial cell replication, and

also contributes to apoptosis. This may have significance for stem cell maintenance, wound healing, and epithelial desquamation. Further studies will be important in identifying the genes involved in this activity. In addition, the DOX-inducible Pax6 system developed herein will be useful to study the role of Pax6 in vivo, and the constructs are now being introduced into transgenic mice.

Acknowledgments

The authors thank Hyun Yi (University of Miami) for general technical assistance.

References

1. Kenyon KR. Anatomy and pathology of the ocular surface. *Int Ophthalmol Clin.* 1979;19:3–35.
2. Tervo T, van Setten GB, Paallysaho T, Tarkkanen A, Tervo K. Wound healing of the ocular surface. *Ann Med.* 1992;24:19–27.
3. Begley CG, Zhou J, Wilson G. Characterization of cells shed from the ocular surface in normal eyes. *Adv Exp Med Biol.* 1998;438: 675–681.
4. Fini ME, Slaugenhaupt SA. Enzymatic mechanisms in corneal ulceration with specific reference to familial dysautonomia: potential for genetic approaches. *Adv Exp Med Biol.* 2002;506: 629–639.
5. Fini ME, Cook JR, Mohan R. Proteolytic mechanisms in corneal ulceration and repair. *Arch Dermatol Res.* 1998;290(suppl):S12–S23.
6. Lu L, Reinach PS, Kao WW. Corneal epithelial wound healing. *Exp Biol Med* (*Maywood*). 2001;226:653–664.
7. Lavker RM, Sun TT. Epithelial stem cells: the eye provides a vision. *Eye.* 2003;17:937–942.
8. Lehrer MS, Sun TT, Lavker RM. Strategies of epithelial repair: modulation of stem cell and transit amplifying cell proliferation. *J Cell Sci.* 1998;111:2867–2875.
9. Wolosin JM, Budak MT, Akinci MA. Ocular surface epithelial and stem cell development. *Int J Dev Biol* 2004;48:981–991.
10. Halder G, Callaerts P, Gehring WJ. Induction of ectopic eyes by targeted expression of the eyeless gene in Drosophila. *Science* 1995;267:1788–1792.
11. Gehring WJ, Ikeo K. Pax 6: mastering eye morphogenesis and eye evolution. *Trends Genet* 1999;15:371–377.
12. Fini ME, Strissel KJ, West-Mays JA. Perspectives on eye development. *Dev Genet* 1997;20:175–185.
13. Wawersik S, Purcell P, Maas RL. Pax6 and the genetic control of early eye development. In: Fini E, ed. *Results and Problems in Cell Differentiation; Vertebrate Eye Development*. Berlin: Springer-Verlag; 2000:16–36.
14. Walther C, Guenet JL, Simon D, et al. Pax: a murine multigene family of paired box-containing genes. *Genomics.* 1991;11:424–434.
15. Tang HK, Singh S, Saunders GF. Dissection of the transactivation function of the transcription factor encoded by the eye developmental gene PAX6. *J Biol Chem.* 1998;273:7210–7221.
16. Sander M, Neubuser A, Kalamaras J, Ee HC, Martin GR, German MS. Genetic analysis reveals that PAX6 is required for normal transcription of pancreatic hormone genes and islet development. *Genes Dev.* 1997;11:1662–1673.
17. Schedl A, Ross A, Lee M, et al. Influence of PAX6 gene dosage on development: overexpression causes severe eye abnormalities. *Cell.* 1996;86:71–82.
18. Koroma BM, Yang JM, Sundin OH. The Pax6 homeobox gene is expressed throughout the corneal and conjunctival epithelia. *Invest Ophthalmol Vis Sci.* 1997;38:108–120.
19. Ton CC, Hirvonen H, Miwa H, et al. Positional cloning and characterization of a paired box- and homeobox-containing gene from the aniridia region. *Cell.* 1991;67:1059–1074.
20. Glaser T, Walton DS, Maas RL. Genomic structure, evolutionary conservation and aniridia mutations in the human PAX6 gene. *Nat Genet.* 1992;2:232–239.
21. Hanson IM, Fletcher JM, Jordan T, et al. Mutations at the PAX6 locus are found in heterogeneous anterior segment malformations including Peters' anomaly. *Nat Genet.* 1994;6:168–173.
22. Davis J, Duncan MK, Robison WG Jr, Piatigorsky J. Requirement for Pax6 in corneal morphogenesis: a role in adhesion. *J Cell Sci.* 2003;116:2157–2167.
23. Collinson JM, Chanas SA, Hill RE, West JD. Corneal development, limbal stem cell function, and corneal epithelial cell migration in the Pax6(+/−) mouse. *Invest Ophthalmol Vis Sci/* 2004;45:1101–1108.
24. Saez E, No D, West A, Evans RM. Inducible gene expression in mammalian cells and transgenic mice. *Curr Opin Biotechnol.* 1997;8:608–616.
25. Duncan MK, Cvekl A, Li X, Piatigorsky J. Truncated forms of Pax6 disrupt lens morphology in transgenic mice. *Invest Ophthalmol Vis Sci.* 2000;41:464–473.
26. Chen J, Huber BT, Grand RJ, Li W. Recombinant adenovirus coexpressing covalent peptide/MHC class II complex and B7–1: in vitro and in vivo activation of myelin basic protein-specific T cells. *J Immunol* 2001;167:1297–1305.
27. Gotz M, Stoykova A, Gruss P. Pax6 controls radial glia differentiation in the cerebral cortex. *Neuron* 1998;21:1031–1044.
28. Warren N, Caric D, Pratt T, et al. The transcription factor, Pax6, is required for cell proliferation and differentiation in the developing cerebral cortex. *Cereb Cortex.* 1999;9:627–635.
29. Warren N, Price DJ. Roles of Pax6 in murine diencephalic development. *Development.* 1997;124:1573–1582.
30. van Raamsdonk CD, Tilghman SM. Dosage requirement and allelic expression of PAX6 during lens placode formation. *Development.* 2000;127:5439–5448.
31. Duncan MK, Haynes JI 2nd, Cvekl A, Piatigorsky J. Dual roles for Pax6: a transcriptional repressor of lens fiber cell-specific beta-crystallin genes. *Mol Cell Biol.* 1998;18:5579–5586.
32. Pearton DJ, Yang Y, Dhouailly D. Transdifferentiation of corneal epithelium into epidermis occurs by means of a multistep process triggered by dermal developmental signals. *Proc Natl Acad Sci USA.* 2005;102:3714–3719.
33. Li T, Lu L. Epidermal growth factor-induced proliferation requires down-regulation of Pax6 in corneal epithelial cells. *J Biol Chem.* 2005;280:12988–12995.
34. Zhou YH, Wu X, Tan F, et al. PAX6 suppresses growth of human glioblastoma cells. *J Neurooncol.* 2005;71:223–229.
35. Liu JJ, Kao WW, Wilson SE. Corneal epithelium-specific mouse keratin K12 promoter. *Exp Eye Res* 1999;68:295–301.
36. Shiraishi A, Converse RL, Liu CY, Zhou F, Kao CW, Kao WW. Identification of the cornea-specific keratin 12 promoter by in vivo particle-mediated gene transfer. *Invest Ophthalmol Vis Sci.* 1998; 39:2554–2561.
37. Zaniolo K, Leclerc S, Cvekl A, et al. Expression of the alpha4 integrin subunit gene promoter is modulated by the transcription factor Pax6 in corneal epithelial cells. *Invest Ophthalmol Vis Sci.* 2004;45:1692–1704.
38. Sivak JM, Fini ME. MMPs in the eye: emerging roles for matrix metalloproteinases in ocular physiology. *Prog Retin Eye Res.* 2002; 21:1–14.
39. Sivak JM, West-Mays JA, Yee A, Williams T, Fini ME. Transcription factors Pax6 and AP-2alpha interact to coordinate corneal epithelial repair by controlling expression of matrix metalloproteinase gelatinase B. *Mol Cell Biol.* 2004;24:245–257.
40. Mohan R, Chintala SK, Jung JC, et al. Matrix metalloproteinase gelatinase B (MMP-9) coordinates and effects epithelial regeneration. *J Biol Chem.* 2002;277:2065–2072.
41. West-Mays JA, Sivak JM, Papagiotas SS, et al. Positive influence of AP-2alpha transcription factor on cadherin gene expression and differentiation of the ocular surface. *Differentiation.* 2003;71: 206–216.
42. West-Mays JA, Coyle BM, Piatigorsky J, Papagiotas S, Libby D. Ectopic expression of AP-2alpha transcription factor in the lens disrupts fiber cell differentiation. *Dev Biol.* 2002;245:13–27.
43. West-Mays JA, Zhang J, Nottoli T, et al. AP-2alpha transcription factor is required for early morphogenesis of the lens vesicle. *Dev Biol.* 1999;206:46–62.

44. Marquardt T, Ashery-Padan R, Andrejewski N, Scardigli R, Guillemot F, Gruss P. Pax6 is required for the multipotent state of retinal progenitor cells. *Cell* 2001;105:43–55.
45. Funderburgh ML, Du Y, Mann MM, SundarRaj N, Funderburgh JL. PAX6 expression identifies progenitor cells for corneal keratocytes. *FASEB J.* 2005;19:1371–1373.
46. Dua HS, Saini JS, Azuara-Blanco A, Gupta P. Limbal stem cell deficiency: concept, aetiology, clinical presentation, diagnosis and management. *Indian J Ophthalmol* 2000;48:83–92.
47. Nishida K, Kinoshita S, Ohashi Y, Kuwayama Y, Yamamoto S. Ocular surface abnormalities in aniridia. *Am J Ophthalmol* 1995; 120:368–375.
48. Sivak JM, Mohan R, Rinehart WB, Xu PX, Maas RL, Fini ME. Pax6 expression and activity are induced in the reepithelializing cornea and control activity of the transcriptional promoter for matrix metalloproteinase gelatinase B. *Dev Biol.* 2000;222:41–54.
49. Lovicu FJ, Steven P, Saika S, McAvoy JW. Aberrant lens fiber differentiation in anterior subcapsular cataract formation: a process dependent on reduced levels of Pax6. *Invest Ophthalmol Vis Sci.* 2004;45:1946–1953.
50. Ren H, Wilson G. Apoptosis in the corneal epithelium. *Invest Ophthalmol Vis Sci.* 1996;37:1017–1025.
51. Lomako J, Lomako WM, Decker SJ, Carraway CA, Carraway KL. Non-apoptotic desquamation of cells from corneal epithelium: putative role for Muc4/sialomucin complex in cell release and survival. *J Cell Physiol.* 2005;202:115–124.
52. Broker LE, Kruyt FA, Giaccone G. Cell death independent of caspases: a review. *Clin Cancer Res.* 2005;11:3155–3162.